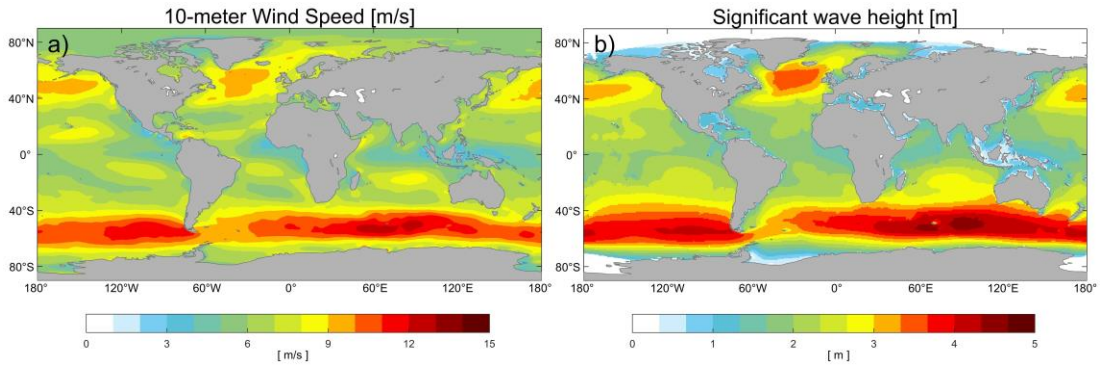

Fig. S1 Annual mean wind speed and significant wave height from 2001 to 2020.

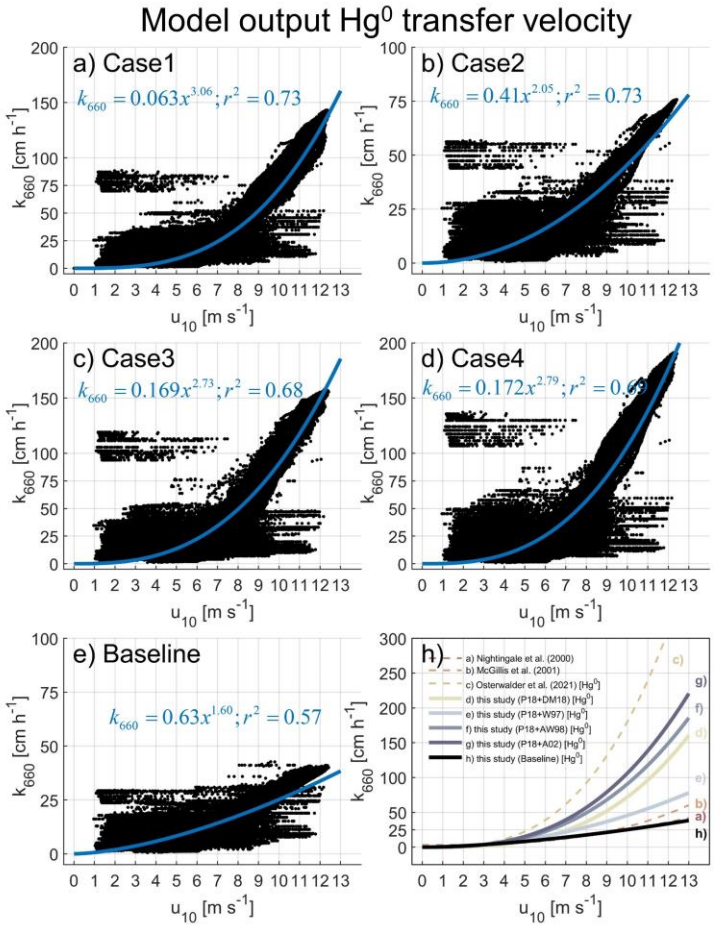

Fig. S2 Wind speed dependence of model output transfer velocities in 2004: a) Case1; b) Case2; c) Case3; d) Case4; e) Baseline. The k-values are normalized to Schmidt number of 660 (20 °C for CO_2 in seawater) and displayed against horizontal wind speed at 10 m [u_{10}]. The blue lines in the figure a-e are the fitting result of the least square method. h) Wind speed dependence of transfer velocities (dash lines are previous studies and solid lines are model outputs). The output transfer velocities show higher values than

calculated results (Figure 3). Because the model also includes the influence of drifting sea ice which will rise kw by increasing shear stress and convectively driven turbulence.

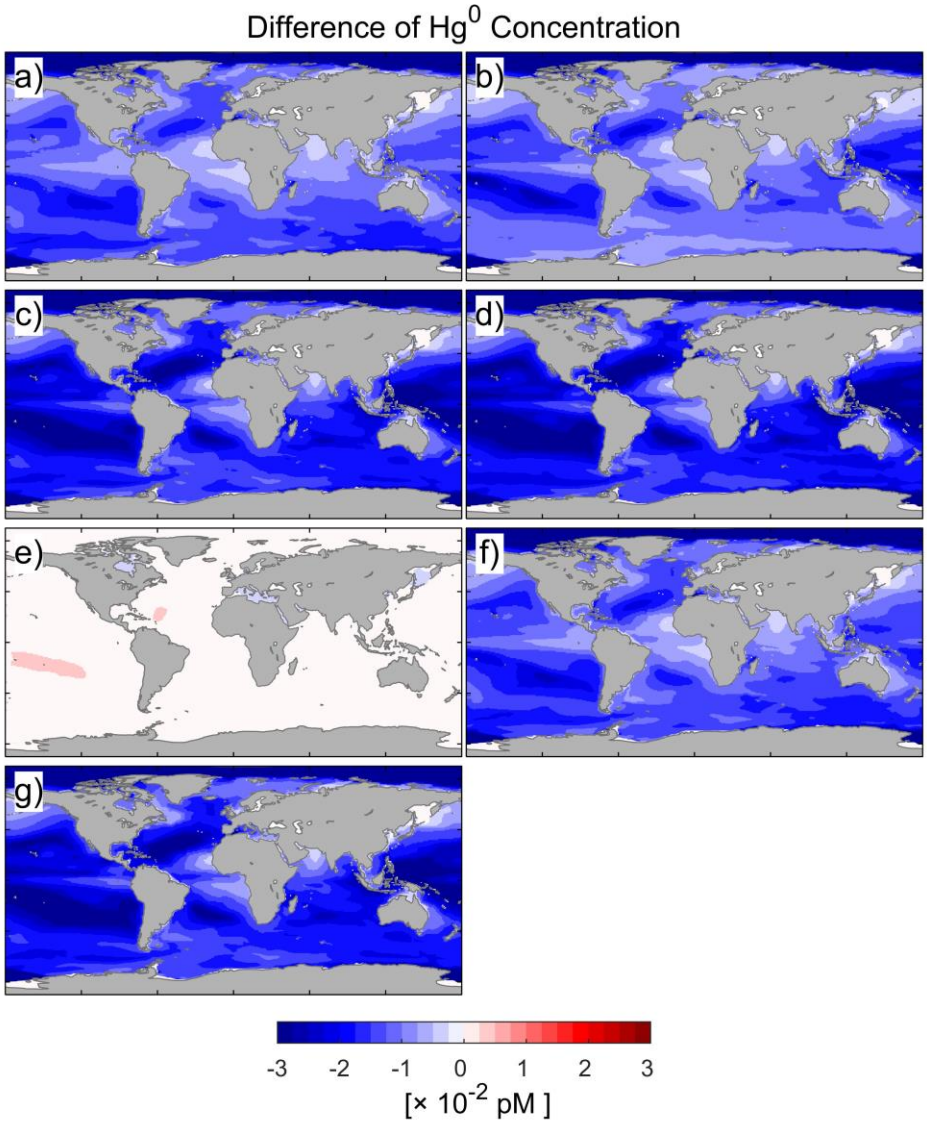

Fig. S3 Difference of annual mean Hg^0 surface concentration with Baseline Model. Panels (a-g) are calculated by Case 1-7.

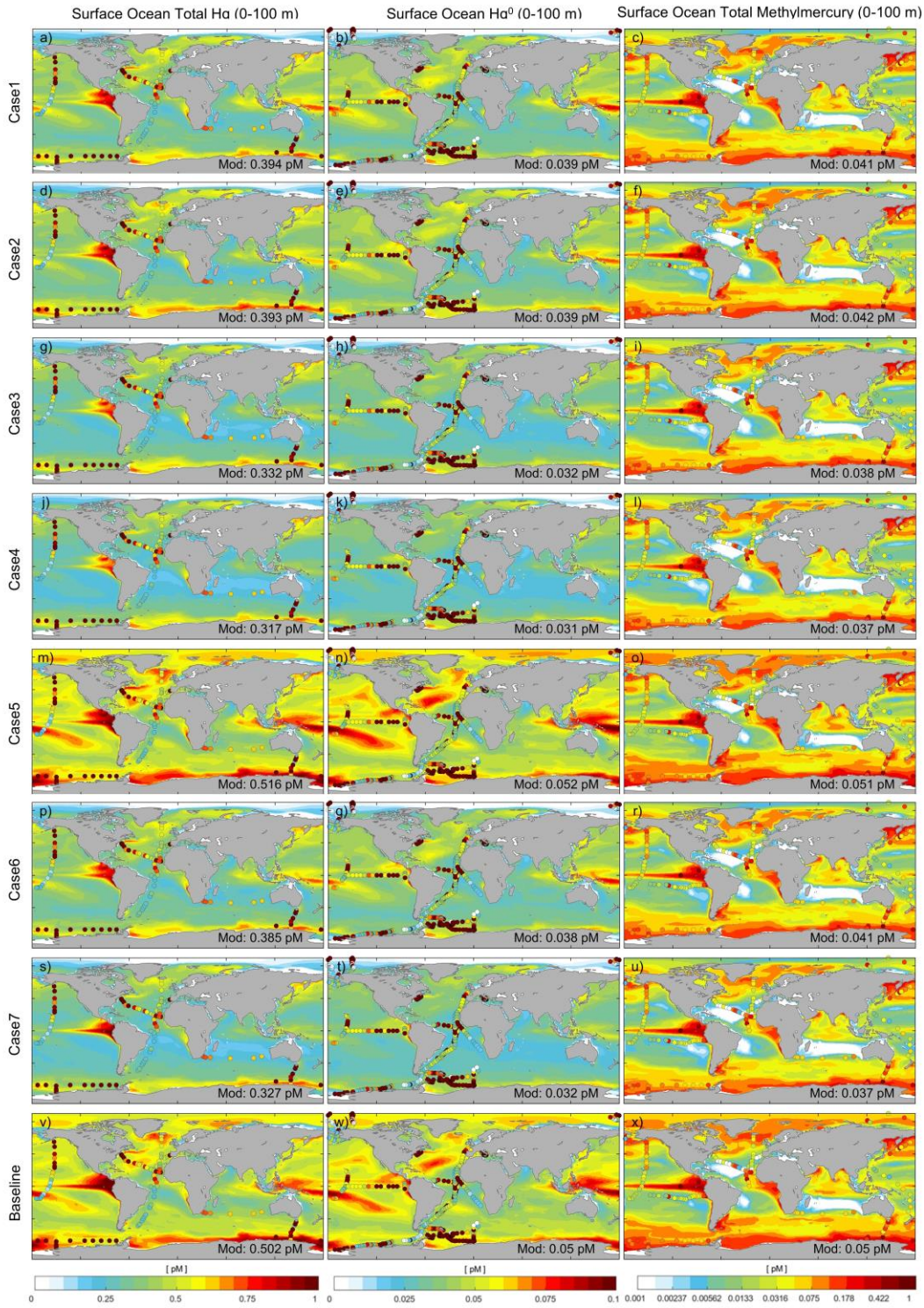

Fig. S4 Comparison between model and observations (filled circles) for Hg abundance in the surface ocean (top 100 m). Comparison against observed seawater total Hg (a, d, g, j, m, p, s, v), Hg^0 (b, e, h, k, n, q, t, w) and MMHg (c, f, i, l, o, r, u, x). The

parameterizations used from the first line to the seventh line are Case1-7 and the last line is Baseline model. Values inset are global mean concentration in unit of pM ($pmol / L$, $pM = 1 \times 10^{-12} mol / L$). The data sources are summarized by Zhang et al.[1]

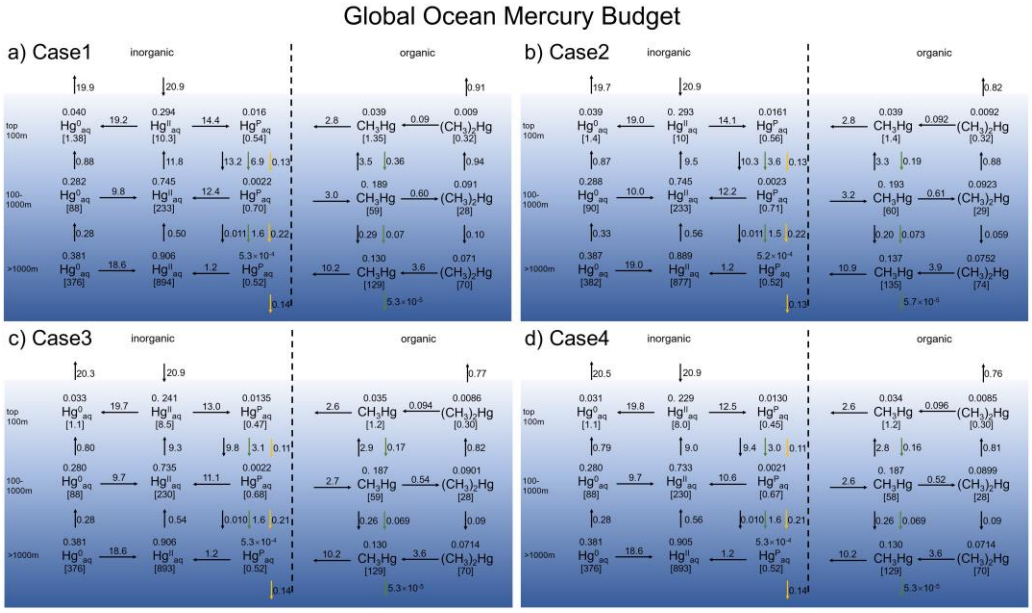

Fig. S5 Hg mass budget for the global ocean. The global ocean is divided into the top 100 m, 100-1000 m, and below 1000 m. Numbers on top of tracer names are average concentrations in units of pM while those below are total masses in units of Mmol. Numbers near arrows are mass flows in units of Mmol/year. The Hg particle sinking and sedimentation fluxes are shown as green and yellow arrows, respectively. a) Case 1; b) Case 2; c) Case 3; d) Case 4.

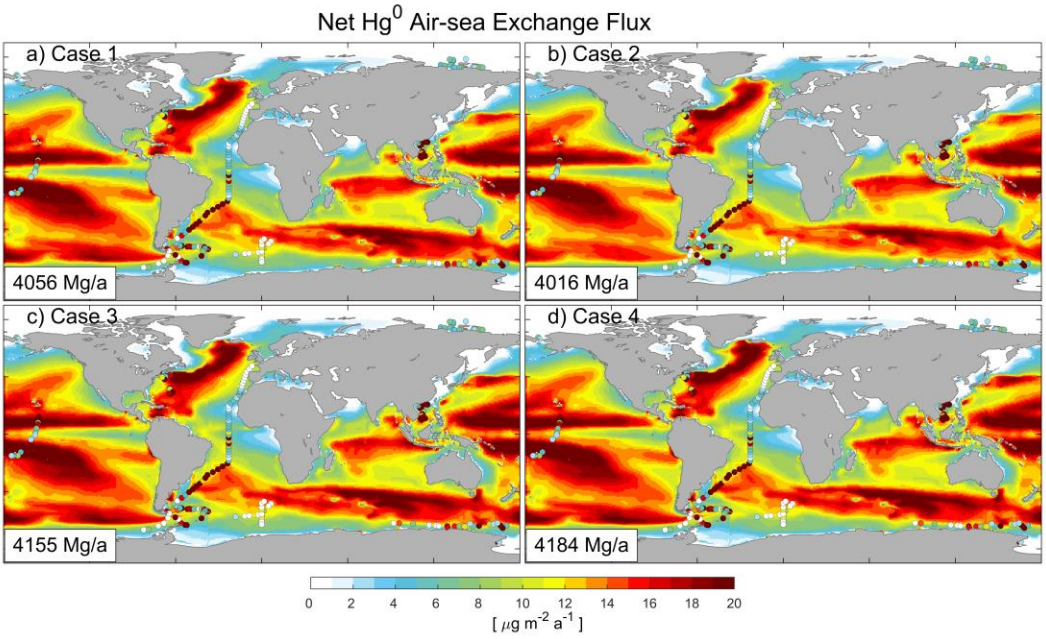

Fig. S6 Comparison between model and observations[2-8] (filled circles) for net Hg^0 air-sea exchange of different parameterization: a) Case1; b) Case2; c) Case3; d) Case4. Values inset are global net atmosphere to ocean transfer flux.

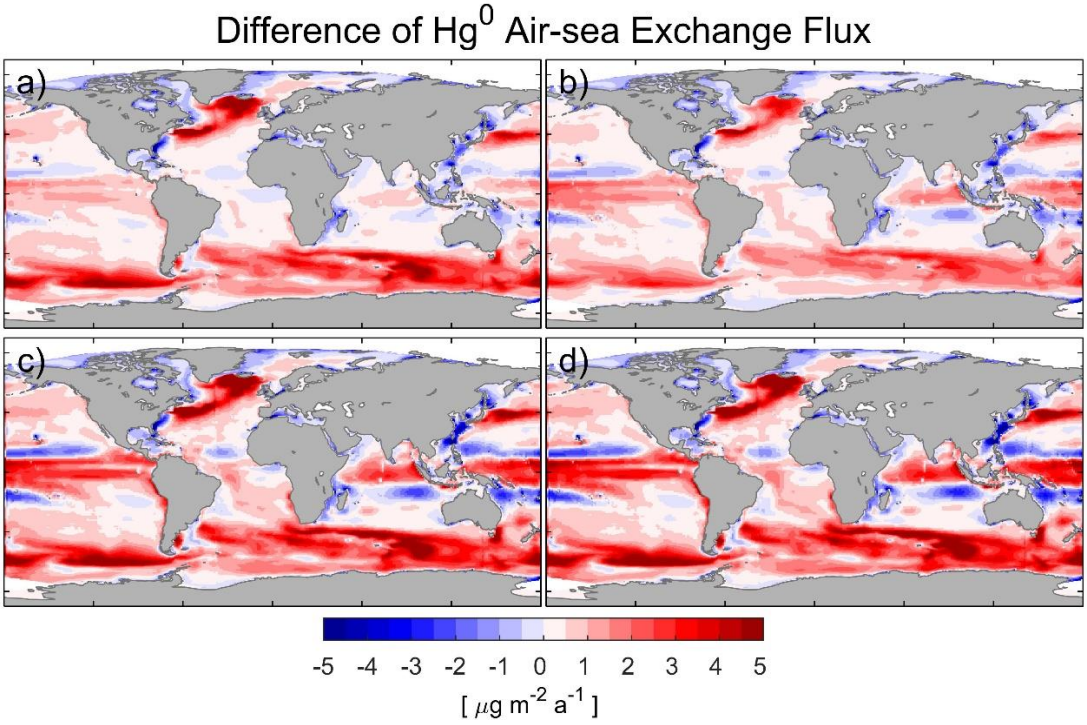

Fig. S7 Difference of annual mean net Hg^0 evasion flux with Baseline Model. Panels (a-d) are simulated by Case 1-4 based upon the combined effect of wave breaking and surfactants.

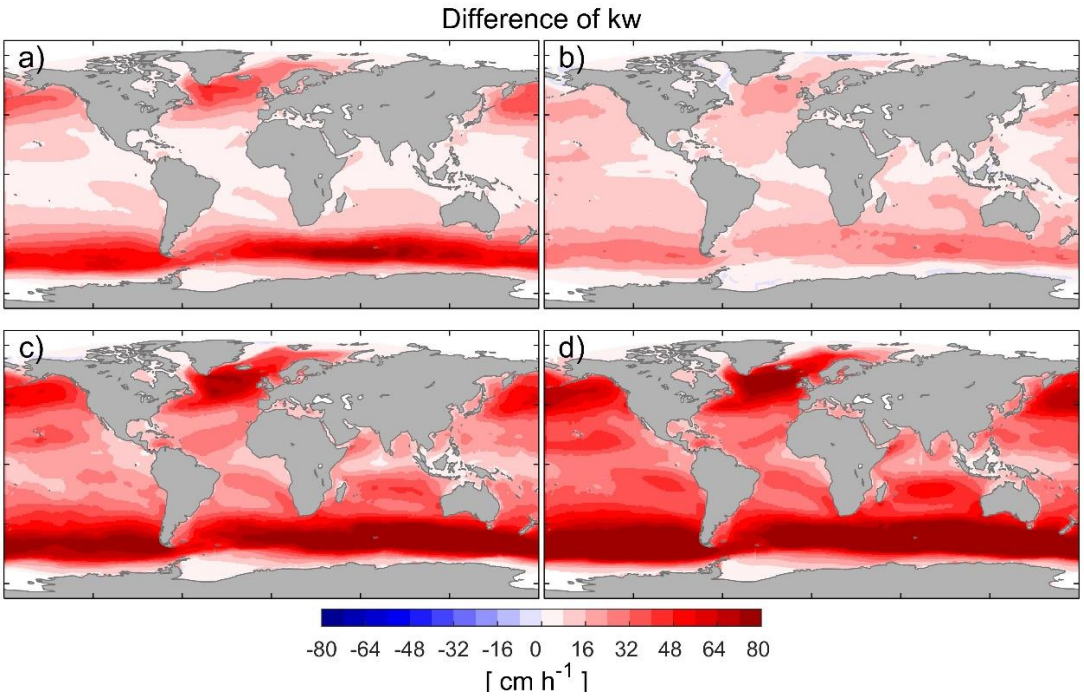

29

30 **Fig. S8** Difference of annual mean transfer velocity with Baseline Model: a) Case1; b) Case2; c) Case3; d) Case4.

31

References

Kalinchuk, V. V., Lopatnikov, E. A., Astakhov, A. S., Ivanov, M. V., and Hu, L.: Distribution of atmospheric gaseous elemental mercury (Hg(0)) from the Sea of Japan to the Arctic, and Hg(0) evasion fluxes in the Eastern Arctic Seas: Results from a joint Russian-Chinese cruise in fall 2018, Science of The Total Environment, 753, 142003, https://doi.org/10.1016/j.scitotenv.2020.142003, 2021.

Kuss, J., Zülicke, C., Pohl, C., and Schneider, B.: Atlantic mercury emission determined from continuous analysis of the elemental mercury sea-air concentration difference within transects between 50°N and 50°S: ATLANTIC Hg SEA-AIR CONCENTRATION DIFFERENCE, Global Biogeochem. Cycles, 25, n/a-n/a, https://doi.org/10.1029/2010GB003998, 2011.

Nerentorp Mastromonaco, M. G., Gårdfeldt, K., and Langer, S.: Mercury flux over West Antarctic Seas during winter, spring and summer, Marine Chemistry, 193, 44–54, https://doi.org/10.1016/j.marchem.2016.08.005, 2017.

Soerensen, A. L., Mason, R. P., Balcom, P. H., and Sunderland, E. M.: Drivers of Surface Ocean Mercury Concentrations and Air–Sea Exchange in the West Atlantic Ocean, Environ. Sci. Technol., 47, 7757–7765, https://doi.org/10.1021/es401354q, 2013.

Soerensen, A. L., Mason, R. P., Balcom, P. H., Jacob, D. J., Zhang, Y., Kuss, J., and Sunderland, E. M.: Elemental Mercury Concentrations and Fluxes in the Tropical Atmosphere and Ocean, Environ. Sci. Technol., 48, 11312–11319, https://doi.org/10.1021/es503109p, 2014.

Wang, C., Wang, Z., Hui, F., and Zhang, X.: Speciated atmospheric mercury and sea–air exchange of gaseous mercury in the South China Sea, Atmos. Chem. Phys., 19, 10111–10127, https://doi.org/10.5194/acp-19-10111-2019, 2019.

Wang, J., Xie, Z., Wang, F., and Kang, H.: Gaseous elemental mercury in the marine boundary layer and air-sea flux in the Southern Ocean in austral summer, Science of The Total Environment, 603–604, 510–518, https://doi.org/10.1016/j.scitotenv.2017.06.120, 2017.

Zhang, Y., Soerensen, A. L., Schartup, A. T., and Sunderland, E. M.: A Global Model for Methylmercury Formation and Uptake at the Base of Marine Food Webs, Global Biogeochemical Cycles, 34, e2019GB006348, https://doi.org/10.1029/2019GB006348, 2020.